

～3. 坪田一男、大鹿哲郎 編集. テキスト  
眼科学. 64-69. 2007

2. 篠田啓. 9. 網膜疾患 A. 黄斑疾患. 1.～  
11. 坪田一男、大鹿哲郎 編集. テキスト  
眼科学. 166-178. 2007

3. 篠田啓. Stargardt 病 (STGD). 眼科  
49:1021-1027, 2007. (黄斑ジストロフィア  
アップデート 編者 岸章治)

4. 篠田啓. 煙草スモッキングはどのく  
らい悪いのか? あたらしい眼科 25:33-37,  
2008. (眼の病—生活習慣病が原因 編者  
岡田アナベルあやめ、坪田一男)

## 2. 学会発表

1. Fujinami K, Tsunoda K, Kazato Y, Shinoda  
K, Miyake Y. Fundus autofluorescence in acute  
zonal occult outer retinopathy (AZOOR).  
Scheperce International Society

2. Imamura Y, Hirasawa M, Hashizume K,  
Noda S, Shirasawa T, Shinoda K, Miyake Y,  
Tsubota K. Characterization of Retinal  
Degeneration in SOD1-Deficient Mice:  
Electrophysiology and Histopathology The  
Association for Research in Vision and  
Ophthalmology, (40th; 2007; Fort Lauderdale,  
Florida). 2007.5

3. Yoshida T, Fujinami K, Shinoda K, Miyake Y,  
Suzuki MT, Terao K, Yoshikawa Y, Iwata T.  
Focal Macular Electroretinogram of  
Cynomolgus Monkey (Macaca fascicularis)  
With Early Onset Macular Degeneration. The  
Association for Research in Vision and  
Ophthalmology, (40th; 2007; Fort Lauderdale,  
Florida). 2007.5

4. Tatar O, Shinoda K, Adam A, Boeyden V,  
Pertile G, Bopp S, Yoeruek E, Eckardt C,  
Bartz-Schmidt KU, Grisanti S. Matrix  
Metalloproteinases in Human Choroidal  
Neovascular Membranes Excised Following

Verteporfin Photodynamic Therapy. The  
Association for Research in Vision and  
Ophthalmology, (40th; 2007; Fort Lauderdale,  
Florida). 2007.5

5. Inomata K, Tsunoda K, Hanazono G,  
Kazato Y, Shinoda K, Miyake Y, Tanifuji M.  
The Distribution of Retinal Responsiveness  
Evoked by Trans-Scleral Electrical Stimulation  
Observed by Intrinsic Signal Imaging in  
Macaque Monkey. The Association for  
Research in Vision and Ophthalmology, (40th;  
2007; Fort Lauderdale, Florida). 2007.5

6. Fujinami K, Hanazono G, Tsunoda K,  
Inomata K, Ohde H, Shinoda K, Miyake Y.  
Fundus Autofluorescence in Occult Macular  
Dystrophy. The Association for Research in  
Vision and Ophthalmology, (40th; 2007; Fort  
Lauderdale, Florida). 2007.5

7. 藤波芳、寺内直毅、花園元、猪俣 公  
一、篠田啓、角田和繁、三宅養三 病巣は、  
網膜? 視神経? 第8回東京レチナクラブ  
2007.3 東京

8. 今村裕、平澤学、橋爪公平、坪田一男、  
白澤卓二、野田節子、篠田啓、三宅養三 SOD1  
欠損マウスの網膜変性の電気生理学的・病  
理学的解析 第111回日本眼科学会 2007.4.  
大阪

9. 藤波芳、寺内直毅、花園元、猪俣公一、  
角田和繁、篠田啓、中村誠、小口芳久、三  
宅養三 夜盲を呈さない小口病の一例 第  
111回日本眼科学会 2007.4.大阪

10. 吉田統彦、藤波芳、篠田啓、三宅養三.  
遺伝性黄斑変性カニクイザル-眼底所見分  
類と黄斑局所網膜電図- 日本網膜硝子体  
学会 2007.11. 第46回 青森

11. 篠田啓 網膜視路疾患の長期観察とそ  
の意義 第55回 日本臨床視覚電気生理  
学会 シンポジウム「網膜・視路疾患の長

期経過」 2007.11 名古屋

12. 木村至、永井紀博、篠田啓、角田和繁、大出尚郎、北和典、小口芳久 不等像視と両眼加算の多局所視覚誘発電位による検討. 第 55 回 日本臨床視覚電気生理学学会 2007.11 名古屋

13. 山田喜三郎、松本惣一セルソ、木許賢一、篠田啓、中塚和夫. 経時的に ERG を検討した Purtscher 網膜症の 1 例. 第 55 回 日本臨床視覚電気生理学学会 2007.11 名古屋

14. 山田喜三郎、木許賢一、河野博文、高木康宏、篠田啓、中塚和夫. Classic 成分の有無によるポリープ状脈絡膜血管症に対する光線力学的療法. 第 61 回 日本臨床眼科学会 2007.10 京都

15. 河野博文、山田喜三郎、木許賢一、高木康宏、篠田啓、中塚和夫. 病的近視の脈絡膜新生血管に対する光線力学的療法. 第 61 回 日本臨床眼科学会 2007.10 京都

16. 藤波芳、花園元、風戸陽子、猪俣公一、角田和繁、篠田啓、大出尚郎、三宅養三. AZOOR の自発蛍光. 第 61 回 日本臨床眼科学会 2007.10 京都

17. 猪俣公一、藤波芳、花園元、角田和繁、篠田啓、大出尚郎、湯沢美都子、三宅養三. 視神経疾患と診断された黄斑部網膜疾患の 3 症例. 第 61 回 日本臨床眼科学会 2007.10 京都

18. 北岡隆、山田浩喜、瓶井資弘、西田健太郎、篠田啓、平形明人. インストラクションコース、硝子体手術手技の XYZ. 第 61 回日本臨床眼科学会、2007.10 京都

19. 池脇淳子、篠田啓、本村由香、中塚和夫、中室隆子、今泉雅資. トリアムシノロンテノン嚢下注射にて発症したと考えられた眼窩膿瘍および眼内炎の 1 例. 第 61 回 日本臨床眼科学会 2007.10 京都

20. 木許賢一、山田喜三郎、河野博文、高木康宏、篠田啓、中塚和夫. 脈絡膜新生血管病変に対する Bevacizumab 併用光線力学的療法の短期成績. 第 61 回 日本臨床眼科学会 2007.10 京都

21. 木許賢一、山田喜三郎、河野博文、高木康宏、篠田啓. 光線力学療法の現状と展望. 第 147 回 大分眼科集談会 2007.6 大分

22. 高木康宏、河野博文、山田喜三郎、篠田啓、中塚和夫、榊保堅. 眼内レンズ挿入を行った虹彩嚢腫の 1 例. 第 147 回 大分眼科集談会 2007.6 大分

23. 高木康宏、岸大地、山田喜三郎、篠田啓、中塚和夫. 当院における最近 10 年間の白内障術後眼内炎の検討. 第 148 回 大分眼科集談会 2007.12 大分

24. 吉田統彦、藤波芳、篠田啓、三宅養三. 遺伝性黄斑変性カニクイザル-眼底所見分類と黄斑局所網膜電図-. 第 46 回 日本網膜硝子体学会 2007.11 青森

#### H. 知的財産権の出願・登録状況

1. 特許取得 なし
2. 実用新案登録 なし
3. その他 なし

厚生労働科学研究費補助金（感覚器障害研究事業）

分担研究報告書

## 網膜内因性信号計測装置性能向上のための設計開発

分担研究者 楠城紹生

株式会社ニデック研究開発本部探索研究部 主席研究員

研究要旨： 本研究は網膜に刺激を与え、その前後での網膜の変化を捉えることにより、非侵襲的に網膜各部位の光に対する神経活動を他覚的に計測することを課題としている。昨年度までは被検者への負担が比較的軽いと言える近赤外光を観察光として用いた研究を中心に進めてきたが、この方法では得られる反応が弱く、生理的にも信号起源が複雑という問題点があった。今年度は上記の研究を進めながら、可視光を用いた比較的反応も大きく信号起源も分かりやすい視細胞の退色反応の研究まで視野を広げて研究を行った。この結果として動物眼(サル)では、比較的単純な手法でS,M,L各錐体細胞が起源と思われる反応を捉えることに成功した。また、人に於いても退色反応と思われる反応を確認することが出来た。しかしこの反応は眼球の動き等による影響を強く受けるため、未だ確度を高める研究が必要不可欠である。

### A. 研究目的

近年、網膜の形態観察をする診断機器は飛躍的に進歩し、3次元的に各細胞層を観察できるようになってきた。これと対照的に、網膜の機能を診断する装置としては自覚的な視力計・視野計の他には、客観的な方法としては電気生理を応用した網膜電図(ERG)しかなく、網膜の機能を空間的に計測するには必ずしも十分とは言えない。

角田らは、最近の脳研究分野における光学計測法という神経活動を捕らえる技術を網膜に応用することを提案し、眼底カメラの利用でその可能性を見出すことに成功。理化学研究所、国立東京医療センター、ニデック社の三者を中心とした研究チームで、全く新しい客観的な網膜機能計測手段の確立を目指すとした。

以上の概要については、当初から同様であり変更はない。

昨年度までは、被検者への負担が比較的軽いと言える近赤外光を観察光として用いた

研究を中心に進めてきたが、この方法では得られる反応が弱く、生理的にも信号起源が複雑という問題点があった。今年度は上記の研究を進めながら、可視光を用いた比較的反応も大きく信号起源も分かりやすい退色反応の研究まで視野を広げて研究を行った。

### B. 研究方法

弊社としては以下の項目（内容）に関わり、主として研究装置開発及び逐次の改良を施すことで研究協力、バックアップを実施する。

#### 1. 近赤外光を用いた内因性信号の計測実験

引き続き従来の内因性信号を計測する実験を行った。

弊社眼底カメラ NM-1000 を改造した装置を用いて、観察光側に IR フィルタ( $\lambda=800\sim 900\text{nm}$ )を挿入して、光刺激前後の動物眼

(麻酔下のサル)の網膜画像の変化を捉えた。ERG との比較およびブロック剤を投与しての実験を角田らがしており、弊社は装置の開発を主に行った。

2. 連続可視光を用いたブリーチング実験  
弊社眼底カメラ NM-1000 を改造した装置を用いて、観察光側に可視フィルタ( $\lambda=560$ 他)を挿入して、動物眼(麻酔下のサル)の網膜画像の変化を捉えた。

可視の連続光の場合、非常に強い羞明感があるが現行の眼底カメラと CCD カメラの構成では感度に限界がある。観察光を下げた実験を行う必要があった為、より感度の高い EM-CCD に取り替えて輝度の低い場合でもブリーチング反応が観察されるか実験を行った。

### 3. 可視のフラッシュ光を用いたブリーチング実験

弊社眼底カメラ AFC-210 を用いて、眼底撮影を繰り返す方法でブリーチング反応の実験を行った。実験対象としては動物眼(麻酔下のサル)およびヒトの実験を行った。

ヒトでは頭蓋骨の固定のためバイトバーを使い、装置内の内部固視灯を固視して眼を安定させた。

#### (倫理面での配慮)

装置の全般的安全性については、以下の国内及び国際安全規格に関わり、研究の実験の進捗段階で特にヒトへの適用に向けてこれらの遵守を前提とした。(JIS T 0601-1、JIS T 0601-1-1、JIS T 0601-1-2、ISO10940、ISO15004)

## C. 研究結果

前記、研究方法の手順に従った進捗状況は以下のとおりである。

1. 赤外光を用いた内因性信号の計測実験  
内因性信号の信号機序について等の研究を角田らが報告している。

2. 連続可視光を用いたブリーチング実験  
比較的安価に入手できる EM-CCD を用いて、減光してのブリーチング実験を行い、

従来の CCD との比較を行った。

EM-CCD の方が観察光を絞っても画像を得ることが出来たが、ショット雑音が非常に大きく、データの信頼性に課題を残す結果となった。

### 3. 可視のフラッシュ光を用いたブリーチング実験

サルでは非常に興味深い結果を得ることが出来た。麻酔により眼が殆ど動かないため、中心窩で非常に強い反応を観察した。また RGB の各色に色分解したところ、赤は S 錐体、緑は M 錐体と桿体、青は S 錐体と桿体と反応と思われる反応の分布を観察することが出来た。

しかしヒトの場合、眼の動きによるアーチファクトや内境界膜からと思われる強い反射光の影響で、サルと同じような反応は得られなかった。しかし、黄斑にブリーチングの反応と思われるものの確認はできた。

## D. 考察

近赤外光を用いた網膜内因性信号の計測については、角田らの研究のサポートで有用だったと考えている。また、サルのブリーチング反応については、中心窩に高い反応を示すトポグラフィーを得ることが出来たが、この分布は解剖学的に知られている桿体細胞と錐体細胞の分布によく類似している。

尚、カメラの RGB のフィルタと SML 各錐体細胞の吸光特性は似たところがあり、乱暴ではあるが RGB 各色情報が各錐体細胞と対応していると考えてそれぞれで差分を求めたが、その結果で赤は L 錐体と思われる中心窩にピークを持つこと、そして黄斑付近にのみに反応が出ていることを確認した。

詳しくは、緑の場合に中心窩に強い反応とそれを囲むように周辺に反応が現れたが、これは M 錐体の主とする反応と Rod-Ring と呼ばれる桿体細胞の反応が混ざって得られたものと推測された。また、青の場合にも緑と似た反応が得られたが、緑の場合に比べて周辺より中心窩に強い反応が現れたが、これは S 錐体を主とする反応と桿体の

反応が得られたものと考えられる。

無論、これだけの実験で各視細胞の反応を捉えたというのは早計だが、比較的簡単な手法で同時に各視細胞の反応を得ることが出来る可能性があると言える。よって、照明や観察系の波長の最適化、明順応や暗順応による変化など撮影手技を研究することにより臨床応用できるのではと考える。

しかし、上記の技術が覚醒下のヒトに利用できなければ意味が無い。そこでバイトバーを用いて頭部を安定させて実験を試みたが、黄斑の反応を確認することは可能であったものの周辺部の反応は記録できなかった。原因はサッカードを含む眼球運動に起因のアーチファクトが感度を大きく低下させていることであり、近赤外光を用いても同じだが、今後の臨床応用にあたっての大きな課題と言える。

#### E. 結論

今年度の研究により、固視がコントロールできれば、比較的簡単に視細胞の退色変化が計測できることが確認できた。また波長や撮影技法を更に研究すれば、各視細胞の反応を同時に計測し、それぞれに分離して計測できる可能性を見出すことが出来た。従来からの近赤外光を用いた内因性信号の計測は、得られる反応が微弱であるため計測が困難であった。そこで今年度は比較的反応の大きい視細胞の退色反応を研究したが、やはり眼の動きに対しては近赤外光での計測と同様に、計測結果に大きく影響することが判明した。

#### F. 健康危険情報

特になし。

#### G. 研究発表

##### 1. 論文発表

ニデックから発表なし

##### 2. 学会発表

ニデックから発表なし

#### H. 知的財産権の出願・登録状況

##### 1. 特許取得

出願済：

「網膜機能測定装置」特願2007-23885

「眼底カメラ」 特願2007-148686

公開中：

「網膜機能測定装置」特開  
2007-319418

「網膜機能測定装置」特開  
2007-319417

「網膜機能測定装置」特開  
2007-319416

「網膜機能測定装置」特開  
2007-319415

「網膜機能測定装置」特開  
2007-319393

「網膜機能測定装置」特開  
2007-202952

「網膜機能測定装置」特開  
2007-151623

「網膜機能測定装置」特開 2007- 89916

「網膜機能測定装置」特開  
2006-239100

「網膜機能測定装置」特開  
2006-136379

##### 3. 実用新案登録

なし

##### 4. その他

なし

### Ⅲ. 研究成果の刊行に関する一覧表

## 研究成果の刊行に関する一覧表

雑誌

発表者氏名	論文タイトル	発表誌名	巻号	ページ	出版年
Hanazono G, Tsunoda K, Shinoda K, Tsubota K, Miyake Y, Tanifuji M	Intrinsic Signal Imaging in Macaque's Retina Reveals Different Types of Flash-induced Light Reflectance Changes of Different Origins	Investigative Ophthalmology & Visual Science	48 (6)	2903-12	2007
Inomata K, Shinoda K, Ohde H, Tsunoda K, Hanazono G, Kimura I, Yuzawa M, Tsubota K, Miyake Y	Transcorneal Electrical Stimulation of Retina to Treat Longstanding Retinal Artery Occlusion	Graefes Arch Clin Exp Ophthalmol	245 (12)	1773-80	2007
Terauchi N, Fujinami K, Shinoda K, Tsunoda K, Hanazono G, Inomata K, Miyake Y	Transient macular dysfunction determined by focal macular electroretinogram	British Journal of Ophthalmology	91 (12)	1709-10	2007
Inomata K, Tsunoda K, Hanazono G, Kazato Y, Shinoda K, Yuzawa M, Tanifuji M, Miyake Y	Distribution of Retinal Responses Evoked by Trans-scleral Electrical Stimulation Detected by Intrinsic Signal Imaging in Macaque Monkeys	Investigative Ophthalmology & Visual Science		in press	2008
Rajagopalan U. M., Tsunoda K, Tanifuji M.	Using the Light Scattering Component of Optical Intrinsic Signals to Visualize in vivo Functional Structures of neural tissues	Dynamic Brain Imaging (Methods in Molecular Medicine). Edited by Farneed Hyder. Humana Press, U.S.			
花園元、柴田尚久、楠城紹生、角田和繁、谷藤学	膜内因性信号測定装置	視覚の科学 (日本眼光学学会誌)	28	31-3	2007
角田和繁	網膜内因性信号計測法—Functional Retinography (FRG)—	日本眼科紀要	58	477—8	2008
風戸陽子、谷藤学、角田和繁	新しい網膜機能のイメージング法—網膜内因性信号計測法—	臨床眼科	62 (3)	227—35	2008
Rajagopalan U, Tanifuji M	Functional optical coherence tomography reveals localized layer-specific activations in cat primary visual cortex in vivo	Optics Letters	32 (17)	2614-6	2007

発表者氏名	論文タイトル	発表誌名	巻号	ページ	出版年
Vidal-Naquet M, Tanifuji M	The effective resolution of correlation filters applied to natural scenes	Proceedings of 2007 IEEE Conference on Computer Vision and Pattern Recognition (CVPR 2007), Beyond Patches Workshop 0 0 IEEE Computer Society USA Minneapolis		1-6	2007
Przybyszewski A, Sato T, Fukuda M	Optical filtering removes non-homogenous illumination artifacts in optical imaging	Journal of Neuroscience Methods	168 (1)	140-45	2008
内田 豪	神経細胞の膜電位がもつ双安定性と状態遷移：その仕組みと情報処理における役割	生物物理	47 (6)	362-7	2007
谷藤 学	ミニ特集「脳における情報処理：時間構造の中に情報を埋め込む」に寄せて	生物物理	47 (6)	352-4	2007
Miyata K, Nakamura M, Kondo M, Lin J, Ueno S, Miyake Y, Terasaki H	Reduction of oscillatory potentials and photopic negative response in patients with autosomal dominant optic atrophy with OPA1 mutations	Invest Ophthalmol Vis Sci	48	820-4	2007
Ikenoya K, Kondo M, Piao CH, Kachi S, Miyake Y, Terasaki H	Preservation of macular oscillatory potentials in eyes with retinitis pigmentosa and normal visual acuity	Invest Ophthalmol Vis Sci	48	3312-7	2007
Hashizume K, Hirasawa M, Imamura Y, Noda S, Shimizu T, Shinoda K, Ozawa Y, Ishida S, Miyake Y, Shirasawa T, Tsubota K	Retinal Dysfunction and Progressive Retinal Cell Death in SOD1-deficient Mice	Am J Pathol		In press	
Kawamura R, Inoue M, Shinoda K, Bissen-Miyajima H	Intraoperative findings during vitreous surgery after implantation of diffractive multifocal intraocular lens	J Ref Cata Surg		In press	



発表者氏名	論文タイトル	発表誌名	巻号	ページ	出版年
Tatar O, Shinoda K, Kaiserling E, Pertile G, Eckardt C, Mohr A, Yoeruek E, Szurman P, Bartz-Schmidt KU, Grisanti S	Early Effects of Triamcinolone Acetonide on VEGF and Endostatin in Human Choroidal Neovascularization	Arch Ophthalmol		In press	
Yokoyama K, Choshi T, Kimoto K, Shinoda K, Nakatsuka K	Retinal circulatory disturbances following intracameral injection of bevacizumab for neovascular glaucoma	Acta Ophthalmol Sca		In press	
Ikwaki J, Imaizumi M, Nakamuro T, Motomura Y, Ohkusu K, Shinoda K, Kimoto K, Nakatsuka K	Fungal Endophthalmitis Developed Following Posterior Subtenon Injection of Triamcinolone Acetonide	Acta Ophthalmol Sca		In press	
Kimoto K, Kishi D, Kono H, Ikwaki J, Shinoda K, Nakatsuka K	Noninvasive morphologic evaluation for retinal astrocytic hamartoma	Acta Ophthalmol Sca		In press	
Sugisaka E, Ohde H, Shinoda K, Mashima Y	Woman with Atypical Unilateral Leber's Hereditary Optic Neuropathy with Visual Improvement	Clin Exp Ophthalmol	35 (9)	868-70	2007
Takaki Y, Nagata M, Shinoda K, Tatewaki S, Yamada K, Matsumoto CS, Hazuku T, Yamashita H, Ikebe T, Nakatsuka K	Severe Acute Ocular Ischemia Associated with Spontaneous Internal Carotid Artery Dissection	Int Ophthalmol		In press	
Ideta S, Noda M, Kawamura R, Shinoda K, Inoue M, Tsubota K	successful Treatment for Subsequent Ptosis after Subtenon Injection of Triamcinolone acetonide	Ophthalmology		In press	
Shinoda K, Rejdak R, Schuettauf F, Blatsios G, Völker M, Tanimoto N, Olcay T, Gekeler F, Lehaci C, Naskar R, Zagorski Z, Zrenner E	Early electroretinographic features of streptozotocin-induced diabetic retinopathy	Clin Exp Ophthalmol	35 (9)	847-54	2007

発表者氏名	論文タイトル	発表誌名	巻号	ページ	出版年
Sato EA, Inoue M, Kimura I, Ohtake Y, Shinoda K	Reduced Chroidal Blood Flow can Induce Visual Field Defect in Open Angle Glaucoma Patients without Intraocular Pressure Elevation following Encircling Scleral Buckling	RETINA		In press	
Inoue M, Shinoda K, Shinoda H, Kawamura R, Suzuki K, Ishida S	Two-step Oblique Incision during 25-gauge Vitrectomy Reduces Incidence of Postoperative Hypotony	Clin Exp Ophthalmol	35 (8)	693-6	2007
Sato EA, Shinoda K, Kimura I, Ohtake Y, Inoue M	Microcirculation in Eyes after Rhegmatogenous Retinal Detachment Surgery	Curr Eye Res	32 (9)	773-9	2007
Torii H, Miyata H, Sugisaka E, Ichikawa Y, Shinoda K, Inoue M	Bilateral Endophthalmitis in Patient with Bacterial Meningitis Caused by Streptococcus pneumoniae	Ophthalmologica		In press	
shinoda H, Nakajima T, Shinoda K, Suzuki K, Ishida S, Inoue M	Jamming of 25-gauge instruments in the cannula during vitrectomy for vitreous haemorrhage	Acta Ophthalmol Scand		Epub ahead of print	
Shinoda H, Shinoda K, Satofuka S, Imamura Y, Ozawa Y, Ishida S, Inoue M	Visual Recovery after Vitrectomy for Macular Hole Using 25-gauge Instruments	Acta Ophthalmol Sca		Epub ahead of print	
Inoue M, Shinoda K, Shinoda H, Suzuki K, Kawamura R, Ishida S	25-gauge cannula system with microvitoretinial blade trocar	Am J Ophthalmol	144 (2)	302-4	2007
Kawamura R, Noda K, Negishi K, Shinoda K, Ishida S, Inoue M, Tsubota K	Intraoperative dehiscence of laser subepithelial keratomileusis (LASEK) flap during retinal detachment surgery	Acta Ophthalmol Scand	85 (4)	459	2007
Nagai N, Ishida S, Shinoda K, Shinoda H, Imamura Y, Noda K, Inoue M	Surgical effect and complications of indocyanine green-assisted internal limiting membrane peeling for idiopathic macular hole	Acta Ophthalmol Scand		Epub ahead of print	
Koto T, Inoue M, Shinoda K, Ishida S, Tsubota K	Residual crystals of triamcinolone acetonide in macular hole may prevent complete closure	Acta Ophthalmol Scand		Epub ahead of print	

発表者氏名	論文タイトル	発表誌名	巻号	ページ	出版年
Tatar O, Adam A, Shinoda K, Yoeruek E, Szurman P, Bopp S, Eckardt C, Bartz-Schmidt KU, Grisanti S	Influence of Verteporfin Photodynamic Therapy on Inflammation in Human Choroidal Neovascular Membranes Secondary to Age-Related Macular Degeneration	Retina	27 (6)	713-723	2007
Sugisaka E, Shinoda K, Ishida S, Imamura Y, Ozawa Y, Nakajima T, Shinoda H, Suzuki K, Kawaguchi N, Inoue M	Patients' Description for Visual Sensations during Pars Plana Vitrectomy under Retrobulbar Anesthesia	Am J Ophthalmol	144 (2)	245-51	2007
Gekeler F, Gmeiner H, Volker M, Sachs H, Messias A, Eule C, Bartz-Schmidt KU, Zrenner E, Shinoda K	Assessment of the posterior segment of the cat eye by optical coherence tomography (OCT)	Vet Ophthalmol	10 (3)	173-8	2007
Tatar O, Adam A, Shinoda K, Eckert T, Scharioth GB, Klein M, Yoeruek E, Bartz-Schmidt KU, Grisanti S	Matrix metalloproteinases in human choroidal neovascular membranes excised following verteporfin photodynamic therapy	Br J Ophthalmol	91 (9)	1183-9	2007
Sailer H, Shinoda K, Blatsios, Kohler K, Bondzio L, Zrenner E, Gekeler F	Investigation of thermal effects of infrared lasers on the rabbit retina: a study in the course of the development of an active subretinal prosthesis	Graefes Arch Clin Exp Ophthalmol	245 (8)	1169-78	2007
Ban Y, Shinoda K, Ohde H, Kaneda E	Enlargement of Optic Nerve Resembling Orbital Mass in Case of Optic Neuritis	Graefes Arch Clin Exp Ophthalmol	245 (6)	911-3	2007
Tatar O, Shinoda K, Adam A, Eckert T, Eckardt C, Lucke K, Deuter C, Bartz-Schmidt KU, Grisanti S	Effect of verteporfin photodynamic therapy on endostatin and angiogenesis in human choroidal neovascular membranes	Br J Ophthalmol	91 (2)	166-73	2007
Watanabe K, Shinoda K, Kimura I, Mashima Y, Ohde H	Dissociation of Conventional Visual field Tests and Multifocal Visual Evoked Potentials in Patients with Hemianopsia	Am J Ophthalmol	143 (2)	295-304	2007

発表者氏名	論文タイトル	発表誌名	巻号	ページ	出版年
玉沖朋子、篠田啓、大出尚郎、小沢洋子、及川亜希子、鈴木浩太郎、石田晋、井上真	黄斑前膜に対する硝子体手術後の網膜感度	眼科	49 (7)	973-7	2007
太田優、鈴木浩太郎、川村亮介、篠田肇、今村裕、小沢洋子、篠田啓、石田晋、井上真	25 ゲージ網膜下注入針を用いた黄斑下手術	眼科	49 (2)	193-8	2007
佐藤裕理、篠田啓、鈴木浩太郎、小沢洋子、石田晋、井上真	酢酸トリアムシノロンのテノン嚢下投与併用光線力学療法	眼科	49 (1)	71-7	2007
篠田啓	視機能検査 I. 網膜電図(ERG), 視覚誘発電位(VEP), 暗順応検査. 1. ~3	テキスト眼科学 坪田一男、大鹿哲郎 編集		64-9	2007
篠田啓	9. 網膜疾患 A. 黄斑疾患. 1. ~11	テキスト眼科学 坪田一男、大鹿哲郎 編集		166-78	2007
篠田啓	Stargardt 病(STGD)	眼科 (黄斑ジストロフィ アップデート 編者 岸章治)	49	1021-7	2007
篠田啓	煙草スモーキングはどのくらい悪いのか?	あたらしい眼科 (眼の病—生活習慣病が原因 編者 岡 田アナベルあやめ、坪田一男)	25	33-7	2008

## IV. 研究成果の刊行物・別刷

# Intrinsic Signal Imaging in Macaque Retina Reveals Different Types of Flash-Induced Light Reflectance Changes of Different Origins

Gen Hanazono,<sup>1,2</sup> Kazushige Tsunoda,<sup>1,2</sup> Kei Shinoda,<sup>1</sup> Kazuo Tsubota,<sup>3</sup> Yozo Miyake,<sup>1</sup> and Manabu Tanifuji<sup>2</sup>

**PURPOSE.** Intrinsic signal imaging is a newly developed technique that can map the neural activity of tissues noninvasively. It has been used to map the functional organization of the retina by recording flash-induced light reflectance changes in the cone and rod photoreceptors. The purpose of this study was to investigate the properties of the intrinsic signals in the monkey's retina. To accomplish this, the intrinsic signals and the electroretinograms (ERGs) evoked by the same stimuli were measured under different recording conditions.

**METHODS.** The fundus of macaque monkeys was observed with infrared light and recorded with a charge-coupled device (CCD) camera. The intrinsic signals were measured as retinal light reflectance changes induced by diffuse or focal flash stimuli. ERGs were recorded under the same stimulating conditions. The reflectance changes induced by different flash intensities, flash intervals, and background luminance were compared.

**RESULTS.** The intrinsic signals were categorized into different groups based on the location in the fundus. Fast signals (peak: ~100 ms) were recorded from the posterior retina including the fovea, and slow signals (peak: 5.0–6.0 seconds) were recorded from the optic disc and nonfoveal posterior retina. The threshold of the slow signal changes was comparable to that of the ERG b-wave, and the thresholds of the fast signals were higher than that of the ERG a- and b-waves.

**CONCLUSIONS.** The retinal intrinsic signals are composed of several components with different response properties and different sources. This recording technique may be useful for mapping the retinal function in eyes with various disorders. (*Invest Ophthalmol Vis Sci.* 2007;48:2903–2912) DOI:10.1167/iov.06-1294

Assessing the functional properties of the retina objectively is essential for making a correct diagnosis and prognosis in various retinal disorders. Although recent advances in imaging techniques—for example, optical coherence tomography

(OCT),<sup>1,2</sup> have revealed the morphologic changes in retinal structures, the functional properties of the retina cannot be evaluated with these imaging techniques. Thus, the electroretinogram (ERG) is still the only practical method of assessing neural activities in the retina.

Intrinsic signal imaging is a well-established imaging technique that translates neural activity into a visual image. This method measures the stimulus-induced light reflectance changes in tissues and has recently been used to assess the cone- and rod-induced retinal responsiveness in macaque monkeys.<sup>3</sup> It has also been used to examine the near-infrared reflectance changes in the human retina<sup>4–6</sup> and optic nerve head.<sup>7</sup> This noninvasive objective technique has good potential for development as a tool for the early detection of retinal dysfunction in cases of age-related macular degeneration, retinitis pigmentosa, and other retinal diseases.

However, before this tool can be brought into the clinic, a detailed knowledge of the properties and origin of the signals obtained by intrinsic signal imaging is necessary. Based on past investigations of intrinsic signal imaging in the cerebral cortex, the decrease in light reflectance (i.e., darkening after a visual stimulus) correlates strongly with local neural activity.<sup>8–11</sup> In the retina, however, the source and the properties of the intrinsic signals appeared to be more complex than in the cerebral cortex due to its complex layered structure.<sup>3</sup>

The purpose of this study was to investigate the basic properties of the retinal intrinsic signals. To accomplish this, we recorded the intrinsic signals of the macaque retina and ERGs under various recording conditions but using the same diffuse flash stimulus. In addition, we recorded the intrinsic signals evoked by focal flash stimuli. The results indicate that the intrinsic signal of the monkey's retina is composed of different components that originate in different layers of the retina.

## METHODS

The procedures used to record the intrinsic signals have been described in detail.<sup>3</sup>

The experiments were performed on two Rhesus monkeys (*Macaca mulatta*) and one Japanese monkey (*Macaca fuscata*). The results from monkeys 1 and 2 are shown in Figures 1 through 5, and those from monkey 3 in Figures 6 and 7. After an intramuscular injection of atropine sulfate (0.08 mg/kg), the monkeys were anesthetized with droperidol (0.25 mg/kg) and ketamine (5.0 mg/kg) and then paralyzed with vecuronium bromide (0.1–0.2 mg/kg per hour). They were artificially ventilated with a mixture of 70% N<sub>2</sub>O, 30% O<sub>2</sub>, and 1.0% to 1.5% of isoflurane. The EEGs, ECGs, expired CO<sub>2</sub>, and rectal temperature were monitored continuously throughout the experiments. Before the recordings, the pupils were fully dilated with topical tropicamide (0.5%) and phenylephrine hydrochloride (0.5%). The experimental protocol was approved by the Experimental Animal Committee of the Riken Institute, and all experimental procedures were performed in accordance with the guidelines of the Riken Institute and the ARVO Statement for the Use of Animals in Ophthalmic and Vision Research.

From the <sup>1</sup>Laboratory of Visual Physiology, National Institute of Sensory Organs, Tokyo, Japan; the <sup>2</sup>Laboratory for Integrative Neural Systems, Brain Science Institute, RIKEN, Saitama, Japan; and the <sup>3</sup>Department of Ophthalmology, Keio University School of Medicine, Tokyo, Japan.

Supported by Researches on Sensory and Communicative Disorders from the Ministry of Health, Labor, and Welfare, Japan.

Submitted for publication October 27, 2006; revised December 28, 2006; accepted March 12, 2007.

Disclosure: G. Hanazono, None; K. Tsunoda, None; K. Shinoda, None; K. Tsubota, None; Y. Miyake, None; M. Tanifuji, None

The publication costs of this article were defrayed in part by page charge payment. This article must therefore be marked "advertisement" in accordance with 18 U.S.C. §1734 solely to indicate this fact.

Corresponding author: Kazushige Tsunoda, Laboratory of Visual Physiology, National Institute of Sensory Organs, Tokyo Japan, 2-5-1 Higashigaoka, Meguroku, Tokyo 1528902, Japan; tsunodakazushige@kankakuki.go.jp.

**Intrinsic Signal Imaging and Data Analysis**

A modified digital fundus camera system (NM-1000; Nidek, Aichi, Japan) was used to observe and measure the light reflectance changes from the ocular fundus. The fundus images were recorded with a charge-coupled device (CCD) camera (PX-30BC; Primetech Engineering, Tokyo, Japan), and the images were digitized with an IBM-compatible computer equipped with a video frame grabber board (gray-level resolution, 10 bits; spatial resolution, 640 × 480; temporal resolution, one-thirtieth of a second; Corona II; Matrox, Quebec, Canada). The camera was focused on the macular vessels, and the area recorded covered 45°, which included the macula, the superior and inferior vascular arcades, and the optic disc. We mainly investigated three retinal sites: the fovea, the posterior retina between the macula and inferior temporal artery, and the optic disc (Fig. 1A).

The fundus was continuously monitored with light from a halogen lamp filtered through an infrared interference filter (840–900 nm). Visible light could not be used for fundus monitoring because the light reflectance changes induced by bleaching of the photopigments have a polarity opposite to that of the intrinsic signals,<sup>3,12–16</sup> leading to incorrect mapping of the stimulus-evoked responses topographically.

Each recording trial consisted of 300 video frames collected at 30 frames per second for a total recording time of 10 seconds. To determine the time course of the flash-induced reflectance changes, we averaged the gray-scale values of 15 video frames collected in 0.5 second for each of the data points (Figs. 1, 6, and 7).

An unfiltered Xenon flash (duration: 1 ms) was given to the whole posterior pole of the ocular fundus or to a focal region of the posterior retina, 500 ms after the initiation of data acquisition. The maximum flash intensity (0-log-unit intensity) measured at the cornea was 308.0 cd · s/m<sup>2</sup> (measured at 50.2 mm from the object lens, by a photoradiometer: model IL-1700; International Light Technologies Inc., Peabody, MA). The timing of the data acquisition and stimulus delivery was under computer control.

Changes in light reflectance from the ocular fundus after the stimulus, such as a darkening (a decrease in light reflectance), and a brightening (an increase in light reflectance), of the retina, were measured. Under infrared observation, the light reflectance of the whole posterior retina decreased (the fundus image became darker) after a flash stimulus (Fig. 1B). The optical signal was calculated as follows: (1) the gray-scale values of the image obtained after the

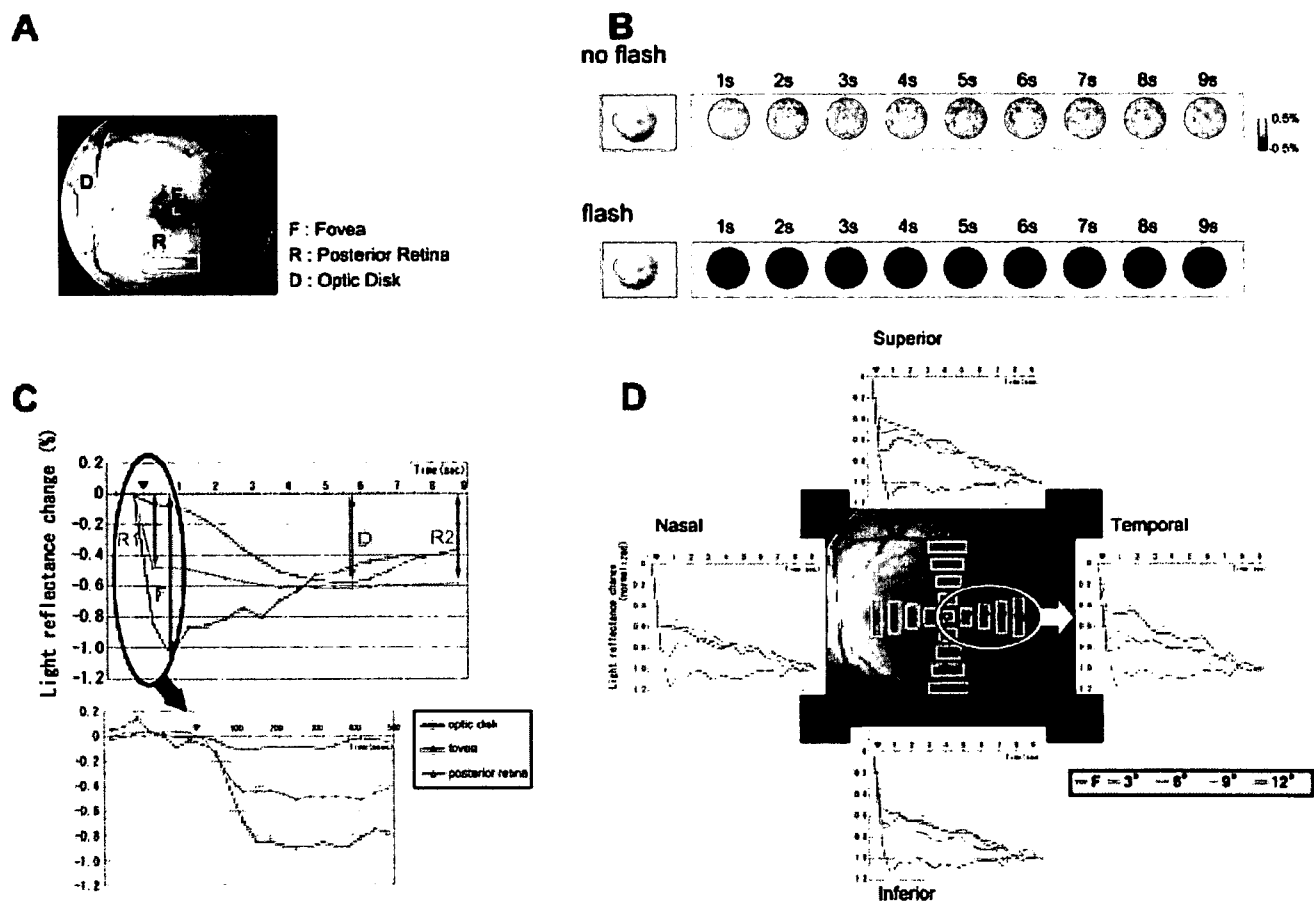


**FIGURE 1.** Fundus photograph and time courses of intrinsic signals after a flash stimulus. (A) Fundus photograph of normal retina showing the regions analyzed. (B) Time courses of two-dimensional images of ocular fundus showing the light reflectance changes during a 10-second trial without (top) and with (bottom) a flash stimulus. Left: fundus images taken at the beginning of a trial; right: light reflectance changes after a flash. Thirty consecutive video frames collected during 1 second were averaged for one poststimulus fundus image. Darkened regions indicate a decrease of light reflectance after the flash stimulus. (C) Plot of the time courses of light reflectance changes in a single trial after a diffuse flash stimulus in the three locations shown in (A). The time after the flash is shown on the abscissa. Arrowhead: point of delivery of the flash. Each point is the average of 15 video frames collected during 0.5 second of the light reflectance changes. Colored arrows: F signal at fovea, D signal at the optic disc and R1 and R2 signals in the nonfoveal posterior retina. The time course of the reflectance changes during the first 500 ms after a flash is shown in the bottom graph where each point is the average of two video frames during one-fifteenth of a second. (D) Time courses of light reflectance changes in a single trial after a diffuse flash, measured at the fovea and four different regions within 12° from the fovea in each quadrant. Amplitudes are indicated as values relative to the light reflectance changes at the end of each trial (1.0). The four regions tested in each quadrant are indicated as distances from fovea (3°, 6°, 9°, and 12°).

stimulus were divided, pixel by pixel, by those obtained during a 0.5-second period before the stimulus, and (2) this ratio was rescaled to 256 levels of gray-scale resolution to show the stimulus-induced reflectance changes.

A deterioration of the signal can be caused by movement artifacts: small involuntary eye movements, blood pressure pulsations, and respiration-associated movements. Eye movements are the most serious artifacts because a different fundus position would be analyzed during the pre- and poststimulus periods. However, these artifacts can be minimized by giving sufficient amounts of muscle relaxants to block eye movements. Pulsations cause small movements of the retinal arteries and optic disc. However, the pulsation-derived reflectance changes are less than one tenth of the stimulus-induced reflectance changes and are almost negligible if 15 video frames are averaged during the 0.5 seconds (Fig. 1C).

Artifacts from respiratory movements produced large light reflectance changes, which were 20% to 40% of the stimulus-induced reflectance changes. This artifact is due to changes in blood flow or volume and periodic back-and-forth movement of the eye, synchronized with the respiration. In our recordings, the respiration-induced artifacts were significant, and the respirator had to be stopped during a recording period of 10 seconds. With the respirator stopped, we could record stable intrinsic signals whose quality was sufficient to map the retinal reflective changes in a single trial without either averaging or offline analysis with realignment of the images.<sup>6</sup>

To measure the time course of the signal changes, we recorded two trials under the same conditions and averaged the results. We found that each trial had to be recorded with at least a 20-minute interval to allow a recovery of the signal production from the previous stimulus. Thus, in experiments where the 11 stimulus intensities were recorded, up to 7 to 8 hours were necessary to record two trials under each condition. Because only two recordings were obtained under each recording condition, the type of statistics that could be used was limited. Unlike ERG recordings, the amplitudes of intrinsic signals are vulnerable to changes in the heart rate, blood pressure, and corneal reflectance. Because it is critical for quantitative comparisons to measure the responses under the same physiological conditions, averaging many trials was impractical for our experimental protocol.

### Electroretinograms

A bipolar contact lens electrode (Mayo, Aichi, Japan) was used to record the ERGs. The ERGs were amplified  $\times 10,000$  and the band-pass filters were set at 0.3 to 500 Hz (Power Lab; AD Instruments, Colorado Springs, CO). A 45° brief white xenon flash stimulus was delivered through the same observation optical system to stimulate the retina while the fundus was monitored with the infrared observation light. As in intrinsic signal imaging, two ERGs were recorded for each recording condition and were averaged.

### Recording Conditions

Initially, we compared the responses of the intrinsic signal images and the ERGs evoked by the same diffuse flash stimulus under different recording conditions: (1) flash intensities (Supplementary Fig. S1; all supplementary figures are online at <http://www.iovs.org/cgi/content/full/48/6/2903/DC1>), (2) flash intervals (Supplementary Fig. S2), and (3) background luminance (Supplementary Fig. S3). Second, we stimulated the retina focally and measured the intrinsic signals in the stimulated and nonstimulated regions.

**Flash Intensity.** The maximum intensity of the xenon flash was  $308.0 \text{ cd} \cdot \text{s/m}^2$ , and neutral density filters were used to attenuate the intensity. The intrinsic signals and ERGs were recorded over an 8.8-log-unit range in 11 steps ( $-8.8$ ,  $-7.8$ ,  $-6.7$ ,  $-6.0$ ,  $-4.8$ ,  $-3.7$ ,  $-3.0$ ,  $-1.8$ ,  $-0.7$ ,  $-0.3$ , and  $0.0$ ). The recordings were performed consecutively with 20 minutes between changes in the intensity under both the dark- and light-adapted conditions. In the light-adapted condition, each recording was followed by 10 minutes of light adaptation. For light adaptation, an 80-mm diameter white polyethylene ball, similar to

a ping-pong ball, was cut in half and placed between the fundus camera and the eye. The ball was illuminated by two halogen lamps through fiber optics so that the luminance in the center was  $30 \text{ cd/m}^2$ . Although the luminance of the ball was not spatially uniform, we believe, that this did not affect the results of the experiments significantly because the luminance at 10° from the center varied by only 94.4% to 103.0% relative to the center (100%). The illuminated ball was removed a few seconds before each recording trial.

**Flash Intervals.** The intrinsic signals and ERGs were recorded after 0.5, 1.0, 3.0, 5.0, 10, 30, and 60 minutes of flash-to-flash intervals. After a 30-minute recovery period, the posterior retina was first bleached by a strong white flash stimulus (bleaching flash:  $-0.3 \text{ log units: } 1.54 \times 10^2 \text{ cd} \cdot \text{s/m}^2$ ), followed by the various interval times listed. The intrinsic signals and ERGs were then measured with a flash (recording flash) of the same intensity as the bleaching flash.

**Background Luminance.** The background luminance was changed from 0 to  $200 \text{ cd/m}^2$  in five steps, to examine the effects of background luminance on the intrinsic signal images. For the intrinsic signal imaging, a strong white flash ( $-0.3 \text{ log units: } 1.54 \times 10^2 \text{ cd} \cdot \text{s/m}^2$ ) was used as a stimulus. For the ERGs, the flash intensity, that evoked the maximum b-wave ( $-3.0 \text{ log: } 3.08 \times 10^{-1} \text{ cd} \cdot \text{s/m}^2$ ) was used.<sup>17</sup> Each recording trial was recorded with a 20-minute interval.

Finally, a focal stimulus was projected onto the retina by inserting a transparent film in the optical pathway of the Xenon strobe. The film was placed at a point that was conjugate to the retina. The shape and size of the stimulus on the retina was determined by the pattern on the film.

## RESULTS

The time course of the intrinsic signals evoked by a brief flash stimulus was different for different regions of the ocular fundus. A representative flash-evoked response from a single trial under dark-adapted condition is shown in Figure 1C. The reflectance changes at the fovea were rapid and reached a negative peak (darkening) within 100 to 200 ms after the flash. The darkening then gradually returned to the prestimulus baseline. The changes in the signals at the optic disc were much slower and reached a peak 5 to 6 seconds after the flash. The signals in the nonfoveal posterior retina were composed of both fast and slow components. The light reflectance decreased rapidly within 100 ms (flexural point) and then gradually decreased, reaching a trough 5 to 6 seconds after the flash. As shown in Figure 1D, the time course of the intrinsic signals of the posterior retina was approximately the same over the whole field except for the small central region within the avascular foveal area (i.e.,  $300 \mu\text{m}$  in diameter).<sup>18</sup> The light reflectance at the fovea did not decrease after the initial negative peak.

There is some evidence that the signal in the nonfoveal posterior retina is composed of at least two components. First, the threshold of the fast and slow signals were different by 4 log units of flash intensity in the dark-adapted condition and 1 or 2 log units in the light-adapted condition, as shown by the following results. Only the later phase of the slow reflectance change was observed after a dim flash stimulus. Second, only the amplitude of the late phase of the signal is vulnerable to changes in the heart rate, whereas that of the early phase is not changed (see the Discussion section).

To analyze the flash-induced intrinsic signals and electrophysiological responses, we used the value of the initial peak of light reflectance change at the fovea (F:  $15 \times 15$  pixels), the value at the flexural point of light reflectance change (R1), or the value at the end of the recording trial (R2) in the inferior retina ( $60 \times 40$  pixels), and the lowest value of light reflectance at the optic disc (D:  $\sim 70 \times 50$  pixels; Fig. 1C).



### Stimulus Intensity

The intrinsic signal images and ERGs recorded after a diffuse flash are shown in Figures 2A, 3A, 4A, and 5A, and the intensities of the intrinsic signals and ERG amplitudes are shown in Figures 2B, 3B, 4B, and 5B.

Under dark-adapted conditions (Fig. 2), the amplitudes of a- and b-waves of the ERGs increased as the stimulus intensity increased.<sup>19</sup> The intrinsic signals of D and R2 had the same threshold as that of the b-wave, and their amplitudes also increased as the intensity increased. The amplitudes of D and R2 reached a plateau at  $-6.0$  log units and did not change significantly with higher intensities. R2 increased again with higher flash intensities over  $-0.3$  log unit in monkey (M)1 and  $-0.7$  log unit in M2.

The threshold of R1 was higher than that of D, R2, and the ERG a-wave. The amplitude of R1 increased gradually with increasing flash intensities. The amplitude of F also increased with increasing flash intensities, but its threshold was higher than that of any of the other intrinsic signals.

Under light-adapted conditions ( $30 \text{ cd/m}^2$ ), the amplitudes of the a- and b-waves increased progressively with increasing flash intensities, but that of the b-wave decreased with intensities higher than  $-3.0$  log units, due to the photopic hill phenomenon (Fig. 3).<sup>17</sup> The thresholds of D and R2 of the intrinsic signal images were higher than those in the dark-adapted condition by 2.1 log units in M1 and 2.8 log units in M2. The thresholds of the D and R2 signals and ERG a- and b-waves were the same in M1.

The threshold of R1 was the same in both dark- and light-adapted conditions. In both conditions, the threshold of F was the same in M1 but was 0.7 log unit lower than that in M2 in the dark-adapted condition. What was striking was that the amplitude of R2 was smaller with brighter flashes in M2 under light-adapted conditions and the light reflectance change became approximately zero at  $-0.3$ -log-unit intensity. There was

a tendency for the amplitude of the R2 signal to decrease with intensities that were 1.0 to 2.0 log units higher than the threshold of the R1 signal.

### Effect of Changes in Flash Intervals

After a bleaching with a bright flash, the amplitudes of the a- and b-waves were reduced and the amplitudes increased with increasing time in the dark (Fig. 4).<sup>20,21</sup> The recovery of the ERG amplitudes appeared slower than that in other studies because our flash intensity was 1.7 log units more intense than that of the ISCEV (International Society for Clinical Electrophysiology of Vision) standard flash.

For the intrinsic signals, only the F signal had a pattern similar to that of the ERGs (i.e., the amplitude increased gradually with longer intervals in the dark after the preceding flash). D, R1, and R2 had peaks at 3 to 5 minutes after the preceding flash, and the amplitudes decreased at 10-minute intervals. These findings indicate that the source of the intrinsic signals of the optic disc and the nonfoveal posterior retina are different from that of the fovea.

### Effect of Background Luminance

The amplitudes of the a- and b-waves decreased progressively as the background illumination increased (Fig. 5).<sup>22,23</sup> The amplitudes of D and R1 of the intrinsic signals under light-adapted conditions ( $10\text{--}200 \text{ cd/m}^2$ ) were 45% to 65% as large as that in the dark-adapted condition in M1 and 60% to 80% in M2. The amplitude of F in the light-adapted condition was approximately 90% as large as that in dark-adapted condition in M1 and 80% to 100% in M2.

In contrast, the R2 signal, was markedly decreased under light-adapted conditions. Even with a weak background of  $10 \text{ cd/m}^2$ , R2 was decreased by approximately 90% in M2, and an increase of 20% in light reflectance was observed in M1. This

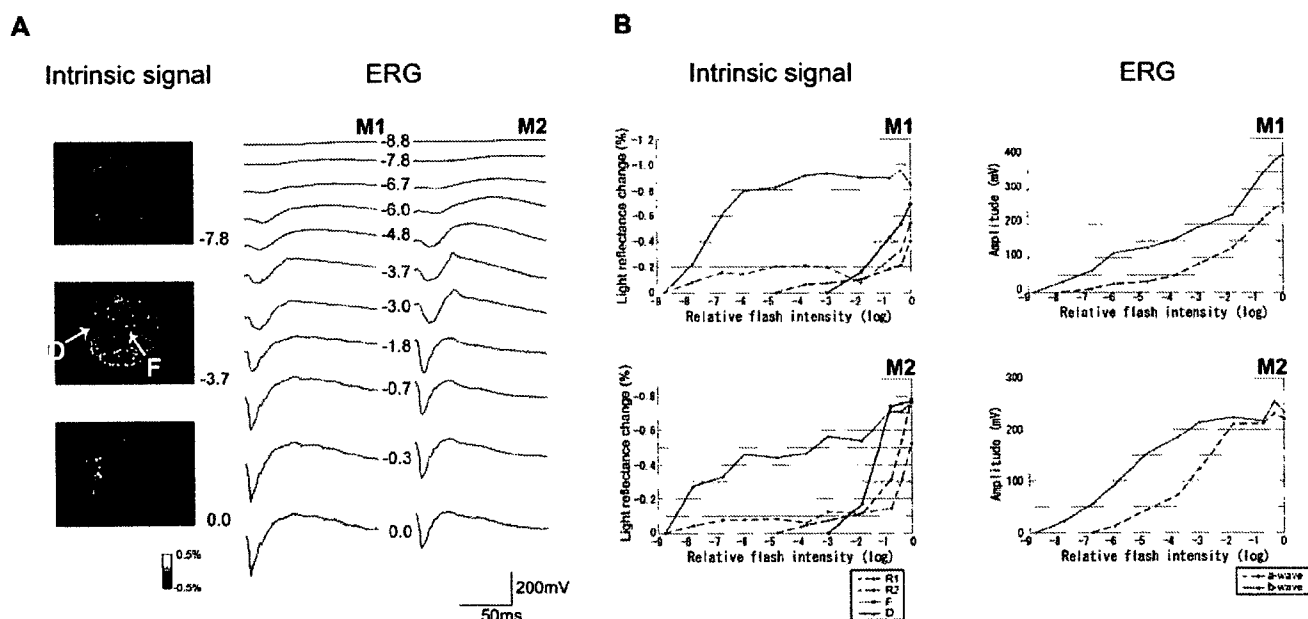


**FIGURE 2.** Intrinsic signal images and ERGs after a diffuse stimulus in dark-adapted conditions. (A) Fundus images of the intrinsic signals (*left*) and ERGs (*right*) after a diffuse flash in the dark-adapted condition with stimulus intensities from  $-8.8$  to  $0$  log units. *Left*: intrinsic signal images from a single trial averaged from 5.0 to 8.0 seconds after the flash. The darkened region in fundus images indicates light reflectance decrease after the flash. The ERGs recorded from monkeys M1 and M2 are shown. The relative log flash intensity responses to the maximum flash are indicated. D: optic disc, F: fovea. (B) *Left*: amplitudes of R1, R2, F, and D of the intrinsic signals in response to increasing flash intensities are shown as light reflectance changes for M1 and M2. *Right*: the amplitudes of the ERG a- and b-waves in response to the same stimulus series. Note that negative values of light reflectance changes are plotted to indicate the strength of intrinsic signals.

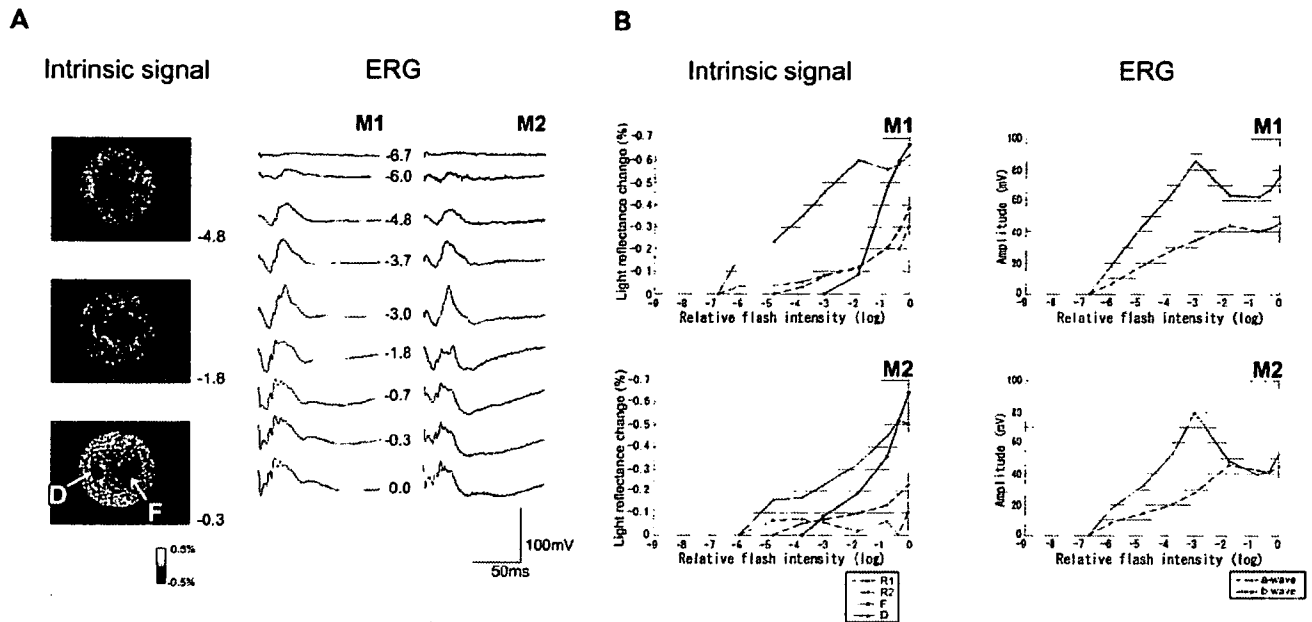


**FIGURE 3.** Intrinsic signals and ERGs after a diffuse stimulation under light-adapted conditions. (A) Fundus images of the intrinsic signals (*left*) and ERGs (*right*) after different stimulus intensities ( $-6.7$ - $0$ -log-unit intensity). Representative signal images for a single trial averaged from 5.0 to 8.0 seconds after a flash are shown. (B) Amplitudes of R1, R2, F, and D of the intrinsic signals and the a- and b-waves of the ERGs in response to various flash intensities are as described in Figure 2.

means that the posterior retina appeared brighter after a flash at the later phase of a recording trial with bright background illumination.

**Responses at Optic Disc**

We have shown that the thresholds of the intrinsic signals at the optic disc were comparable to the threshold of the ERG b-waves and that even a dim stimulus can evoke a strong signal

at the optic disc (Fig. 2). To determine the contribution of blood-related changes to the intrinsic signals at the optic disc, we measured the responses from different regions within the optic disc (Fig. 6A): (1) the central region where the central retinal artery and vein run perpendicular to the imaging plane (Center), (2) over the superior branch of the central retinal artery (Artery), (3) over the superior branch of the central retinal vein (Vein), (4) temporal and nasal regions where large

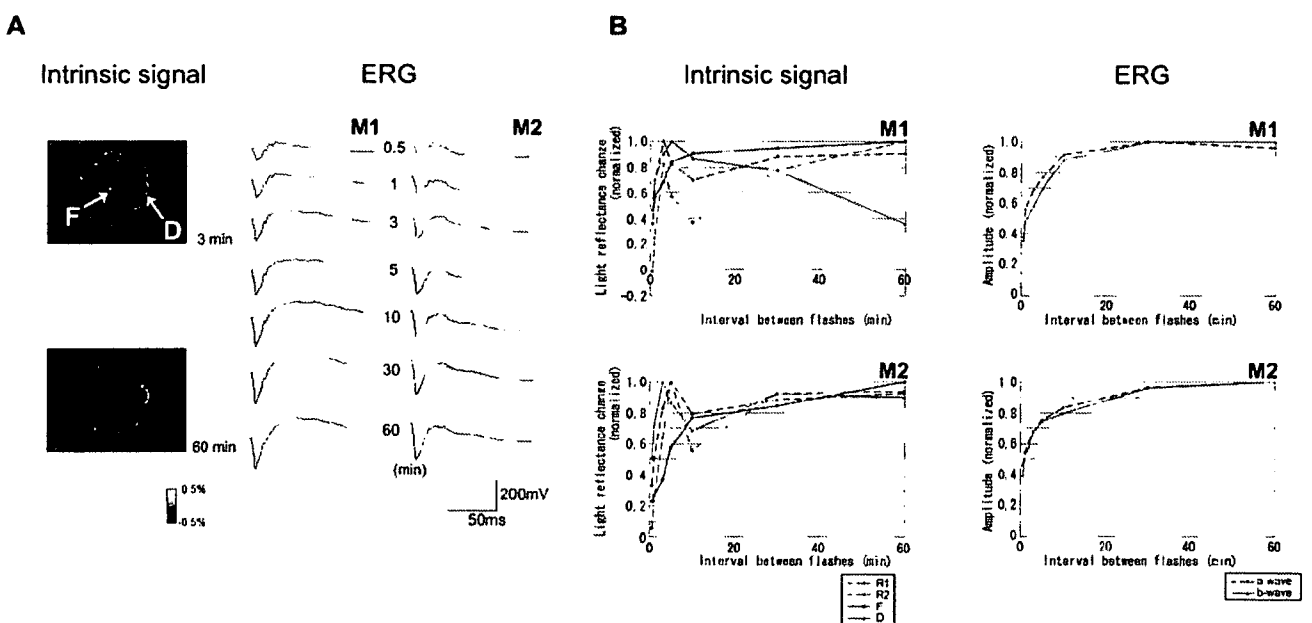


**FIGURE 4.** Intrinsic signals and ERGs after a diffuse stimulus recorded at different times after bleaching. (A) Fundus images of intrinsic signals (*left*) and ERGs (*right*) evoked by a diffuse flash ( $-0.3$  log unit) at different intervals (0.5-60 minutes) after a bleaching flash at the same intensity. Representative images from a single trial averaged from 5.0 to 8.0 seconds after a flash are shown. (B) Amplitudes of R1, R2, F, and D of the intrinsic signals and a- and b-waves of the ERGs at different flash intervals. Amplitudes are relative to the maximum for each signal component.

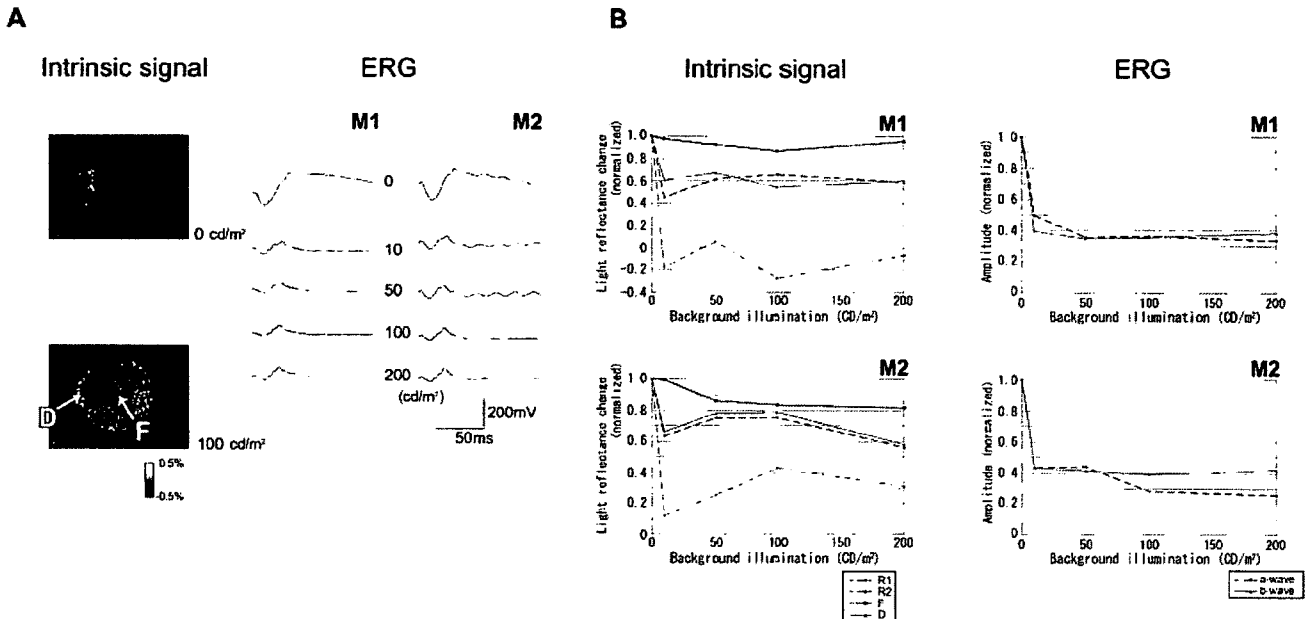


**FIGURE 5.** Intrinsic signal images and ERGs after a diffuse flash stimulus on different background luminances. (A) Fundus images of intrinsic signals (left) and ERGs (right) after a diffuse flash on different background luminances (0–200 cd/m<sup>2</sup>). Representative signal images in a single trial averaged from 5.0 to 8.0 seconds after a flash (–0.3 log unit) are shown. For the ERGs, a flash with the maximum intensity which evoked a b-wave without photopic hill phenomenon was used (–3.0 log units). (B) Amplitudes of R1, R2, F, and D of the intrinsic signals and the ERG a- and b-waves with different background luminances. Amplitudes are relative to the maximum for each signal component.

vessels are not present (Temporal and Nasal), and (5) the entire optic disc (D). A diffuse flash of –0.7 log unit intensity was used for stimulation, and 17 consecutive trials with 3-minute intervals were averaged.

The light reflectance changes were especially large in the central region where the central retinal artery and vein pass through the optic nerve (three times larger than that in the whole region; Fig. 6B). The light reflectance changes over the superior branch of the central retinal artery and vein were 1.2 times larger than that of the whole region. Although the size of the intrinsic signals varied in different regions within the margins of the optic disc, the time course at each region seemed to be almost the same (Fig. 6C).

**Focal Stimulation**

The recording of the focal macular ERG is a technique used to measure the electrical responses in the macula by focally stimulating the macular region.<sup>24,25</sup> Focal flash stimuli can be given to the posterior retina with our recording system, however, our system is not setup to deliver a background illumination to suppress the rod responses and cannot measure the electrical activity in the stimulated region. We have stimulated focal regions of the posterior retina, and compared the time course of the intrinsic signals in both the stimulated and nonstimulated regions in dark-adapted conditions.

First, the macular area including the fovea was focally stimulated with an 8.8° circular stimulus (Figs. 7A, 7B). The light

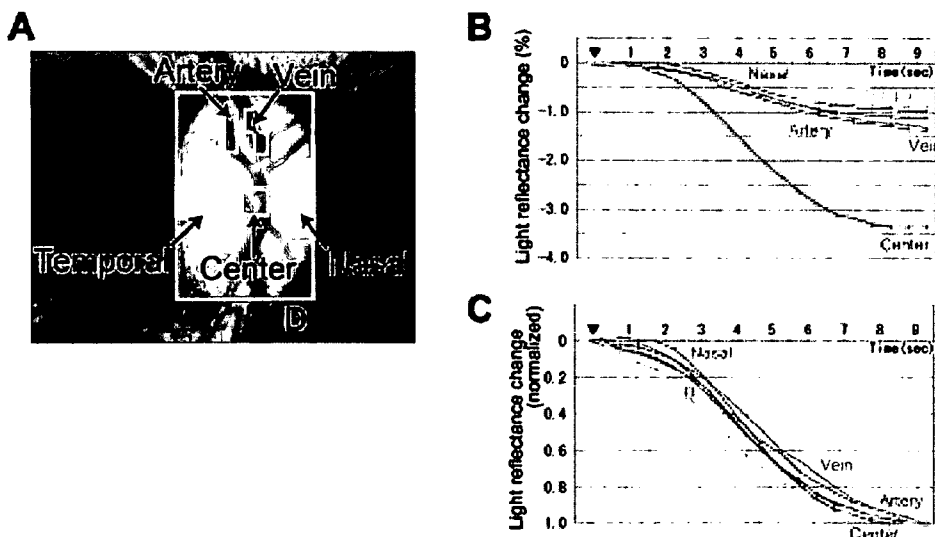


**FIGURE 6.** Time courses of intrinsic signals evoked by a diffuse flash from six regions of the optic disc. (A) Photograph of the optic disc showing the areas measured. D, entire optic disc; Center, central region where central retinal artery and vein run perpendicularly to the imaging plane; Artery, superior branch of central retinal artery; Vein, superior branch of central retinal vein; Temporal, temporal region, where large vessels are not present; and Nasal, nasal region, where large vessels are not present. (B) Plot of the time courses of the intrinsic signals measured at the six regions of the optic disc, presented as absolute values in light reflectance changes. (C) Plot of the time courses of the intrinsic signals, presented as relative to the maximum for each recording region.

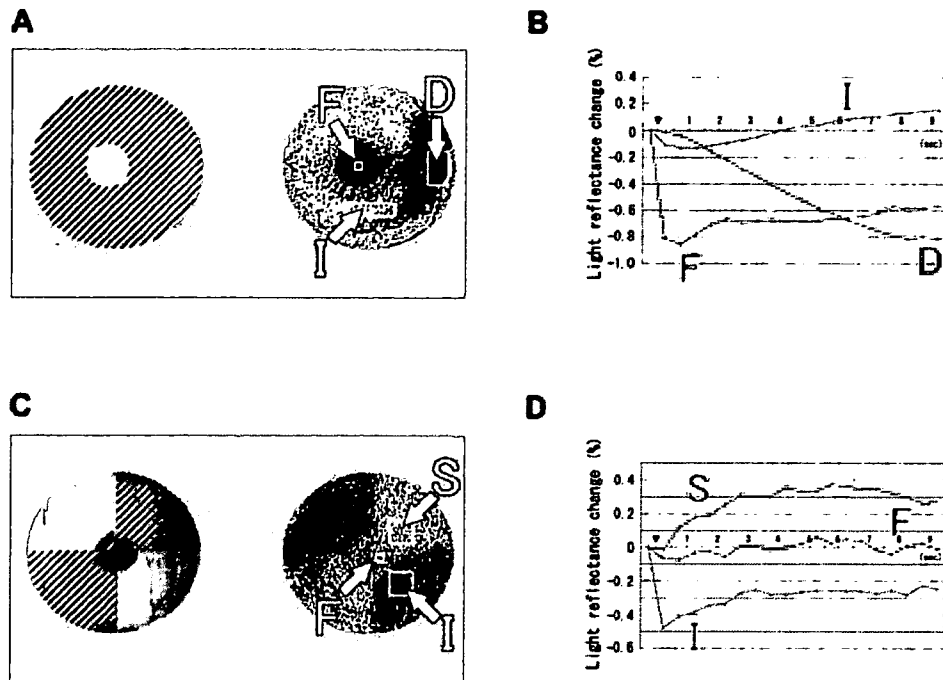


**FIGURE 7.** Effect of focal stimulus on the intrinsic signals. (A) *Left:* fundus image showing circular focal stimulus in the macula including the fovea (8.8° in diameter). The stimulus was blocked over the *hatched area*. Regions for time course analysis are indicated as F (fovea), D (optic disc), I (inferior retina within the vascular arcade, sparing thick vessels). *Right:* fundus image of intrinsic signal evoked by the focal stimulus, averaged from 6.5 to 9.5 seconds after stimulation. Data from four consecutive trials were averaged. (B) Plot of the time courses of light reflectance changes in a single trial after a focal flash at the three locations shown in (A). (C) *Left:* fundus image showing mosaic-like focal stimulus in the posterior pole, sparing central 8.0° including fovea. Regions for time course analysis are indicated as F (nonstimulated fovea), S (stimulated superior retina), and I (nonstimulated inferior retina). *Right:* two-dimensional image of intrinsic signal evoked by the focal stimulus, averaged from 6.5 to 9.5 seconds after stimulation (single trial). (D) Plot of the time courses of light reflectance changes in a single trial after a focal flash at the three locations shown in (C).

reflectance in the stimulated region decreased (Fig. 7B; F) and the region that darkened exactly matched the location of the stimulus (Fig. 7A). In contrast, the region without stimulation became brighter at the later phase of a recording trial (Fig. 7B; D). When two quadrants of the posterior retina were stimulated with the macula spared, the intrinsic signal showed exactly the same darkening pattern as the shape of the stimulus (Fig. 7C). The stimulated posterior retina (I) showed a negative R1 and negative R2 signal (i.e., a darkening; Fig. 7D). The nonstimulated area of the posterior pole (S) was brighter (positive R2), which is usually not observed under other recording conditions. The fovea (F), where the stimulus was masked, did not show any light reflectance changes after the flash.

## DISCUSSION

The origin of the intrinsic signals in the cerebral cortices has been extensively investigated; however, most of the studies have dealt with the deoxygenation of hemoglobin.<sup>8,9,11</sup> The standard hypothesis is that the intrinsic signals in the cerebral cortex arise from light reflectance changes due to the many metabolic changes after neural activation. For example, the intrinsic signal measured at 570 nm is dominated by changes in the blood volume in the capillaries: That at 600 to 650 nm is dominated by the changes in the deoxygenation level of hemoglobin, and that in the infrared region is dominated by changes in tissue light scattering. Although different metabolic changes are highlighted at different wavelengths, the optical

responses obtained at these wavelengths had nearly the same spatial pattern of activation as that of the activated neurons.<sup>9,26</sup> Whatever wavelength was chosen for the measurement of reflectance, the most critical premise for evaluating the intrinsic signal has been that it is the darkening (i.e., a decrease in light reflectance), that correlates with the local neural activity. This is more or less true of the intrinsic signal images in the retina<sup>3</sup>; however, the spatial distribution of the signals appeared to be more complicated when the retina is focally stimulated.

Our goal was to find out what each signal component represented by comparing the intrinsic signals with the ERGs recorded under the same conditions. Although the spatially localized responses of the intrinsic signals cannot be directly compared with the responses in full-field ERGs, this comparison may provide us with some keys to determine the possible mechanisms of the production of the intrinsic signals, because the neuronal mechanisms of the production of the ERGs have been well investigated.

It is important to understand that, in principle, the intrinsic signals are not necessarily produced by photoreceptors: There may be differences in the site of the photoreceptor and the site for producing the signals. The light reflectance changes reflect the summation of the stimulus-evoked metabolic changes happening in the 10 retinal layers, each of which may produce signals with different characteristics. The same difficulty arises when the origin of the different components of the ERGs is investigated. Thus, the type of activated photoreceptors and